Physics and Chemistry of Fission

1973

Volume 2

PROCEEDINGS SERIES

PHYSICS AND CHEMISTRY OF FISSION

1973

PROCEEDINGS OF THE THIRD IAEA SYMPOSIUM
ON THE
PHYSICS AND CHEMISTRY OF FISSION
HELD BY THE
INTERNATIONAL ATOMIC ENERGY AGENCY
IN ROCHESTER, NEW YORK, 13-17 AUGUST 1973

In two volumes

VOL. II

INTERNATIONAL ATOMIC ENERGY AGENCY
VIENNA, 1974

FOREWORD

This third international Symposium on the Physics and Chemistry of Fission, held in Rochester, N.Y., from 13 to 17 August 1973, was a worthy successor to the important symposia held in Salzburg (1965) and in Vienna (1969). Although there may not have been in Rochester quite the excitement that prevailed in Vienna (where the beautiful verification of the structured fission barrier provided by the Strutinsky calculations was presented), the present meeting reaped the benefits of this revolutionary discovery. The first direct experimental verifications of the deformed fission isomers have also only recently been achieved.

The present Symposium, somewhat more than previous ones, concentrated on theoretical concepts and calculations concerning the fission process itself, and only on those new experimental results most pertinent to the theoretical development. Contained in these two volumes are the full texts and discussions of the 62 papers presented at the Symposium, and abstracts of those contributions that, because of time limitations, could not be presented.

These Proceedings of course do not represent the *last* word on this obviously complex topic. It is apparent that even the liquid drop features of the fission process have not yet been fully, or even adequately, worked out, the most obvious deficiency still being a reliable treatment of the dynamics, where a better knowledge of the 'viscosity' is obviously needed. The importance of quantum mechanical, single particle effects in the fission process is emphasized in these Proceedings, and a number of advances in microscopic calculations are included.

It is clear, in view of the large participation and the quality of the work presented, that scientists throughout the world find these meetings a valuable international forum for the exchange of information and welcome the Agency's initiative in promoting this continuing series of symposia.

EDITORIAL NOTE

The papers and discussions incorporated in the proceedings published by the International Atomic Energy Agency are edited by the Agency's editorial staff to the extent considered necessary for the reader's assistance. The views expressed and the general style adopted remain, however, the responsibility of the named authors or participants.

For the sake of speed of publication the present Proceedings have been printed by composition typing and photo-offset lithography. Within the limitations imposed by this method, every effort has been made to maintain a high editorial standard; in particular, the units and symbols employed are to the fullest practicable extent those standardized or recommended by the competent international scientific bodies.

The affiliations of authors are those given at the time of nomination.

The use in these Proceedings of particular designations of countries or territories does not imply any judgement by the Agency as to the legal status of such countries or territories, of their authorities and institutions or of the delimitation of their boundaries.

The mention of specific companies or of their products or brand-names does not imply any endorsement or recommendation on the part of the International Atomic Energy Agency.

CONTENTS OF VOL. II

MASS, CHARGE AND KINETIC ENERGY DISTRIBUTIONS IN FISSION

(Session VI)

SYMMETRIC AND ASYMMETRIC FISSION OF Ra- AND Ac-ISOTOPES

E. KONECNY, H.J. SPECHT, J. WEBER
Beschleunigerlaboratorium der
Universität und Technischen Universität München,
Munich, Federal Republic of Germany

Abstract

SYMMETRIC AND ASYMMETRIC FISSION OF Ra- AND Ac-ISOTOPES.

Fission probabilities and fragment anisotropies have been investigated at low excitation for fission of ^{226}Ac, ^{227}Ac, ^{228}Ac and ^{225}Ra, ^{227}Ra induced on a ^{226}Ra target by direct reactions with a 23.5-MeV ^{3}He beam and an 18-MeV d beam. These results show that the triple-humped character of the mass distribution pertains to low excitation energies where second- and higher-chance fission are energetically excluded. More important, they reveal different thresholds for symmetric and asymmetric fission. In addition, the angular anisotropies for both components close to the fission barrier seem to be different, also suggesting that asymmetric and symmetric fission of the nuclei investigated proceed over different saddle points. The fission probability Γ_f/Γ_n increases exponentially for both components, with a much bigger slope for the symmetric one. For ^{227}Ra and ^{228}Ac the fission probability for symmetric fission even exceeds that for asymmetric fission already at some few MeV above the barrier.

The average kinetic energy is lower for the symmetric than for the asymmetric component and does not change significantly with excitation energy of the fissioning nucleus. On the contrary, for asymmetric fission it decreases with excitation, as observed for fission of actinide nuclei.

1. INTRODUCTION

One of the important problems in nuclear fission has been to understand the existence of two types of fragment mass distributions, symmetric and asymmetric. Low excitation fission of higher-Z actinide nuclei is typically asymmetric (for a review see, e.g. ref.[1]), characterized by a double humped mass distribution. On the contrary, nuclei near Pb and Bi exhibit a symmetric mass distribution [2,3]. For fission of nuclei in the intermediate region (Ra, Ac, Th, Pa) a triple humped mass distribution with well-established minima between the three mass yield peaks is observed[4-11].

It has been suggested that the triple humped mass distribution is the result of a superposition of two different fission components, a symmetric one which has similar features like the symmetric fission of lighter nuclei and is appropriately described by the liquid drop model[12] and an asymmetric component, which shows the same characteristic features like fission of U or Pu, the energetics of which is explained to very great detail by the influence of shells in the nascent heavy fragment [13].

Briefly summarized, the evidence for two separate components is the following: (a) The average total fragment kinetic energy for symmetric fission is about 5 MeV smaller than for asymmetric fission; the average values for the

asymmetric and symmetric component follow separately the kinetic energy systematics of asymmetric fission for nuclei with higher Z and of symmetric fission for lower-Z nuclei, respectively[5]. (b) The dependence of the fragment kinetic energy on the excitation energy of the fissioning nucleus is very different for the two components (see below). (c) If analyzed as a function of fragment mass, the width of the kinetic energy distribution shows clear maxima for those fragment masses for which the contribution of both components is about equal; apparently, another contribution is added to the "intrinsic" energy width of each component which results from the difference in average values[5,9]. (d) The fragment excitation energy as represented by the number of evaporated neutrons shows independent evidence for the superposition of two components, becoming especially visible in the number of emitted neutrons as a function of fragment kinetic energy for constant mass ratio. A full and quantitative description is given in ref.[9].

Although there are hints for two components even for U and Pu fission at moderate excitation energies[6] they become most clearly visible for Ra or Ac. Since so far all experiments exhibiting evidence for two-component fission were carried out at higher excitation energies, it remained experimentally undecided whether the two components are associated with two different fission barriers. According to recent calculations on the deformation-dependent nuclear potential energy surface[14-18], the character of the fragment mass split is, in fact, explained as a consequence of either an asymmetrically (pear shape like) or a symmetrically distorted outer fission barrier, with slight hints even for two different saddles in the same nucleus[14,15].

It therefore seemed desirable to measure the fission probability and the fragment anisotropy (presumed to be determined at the barrier) close to the fission threshold, separately for the two mass components. Such a study is not feasible for higher-Z actinide nuclei both because of the inner barrier being the higher one[15] and the extremely low relative yield ($< 10^{-3}$) of the symmetric component close to the barrier; earlier attempts in this direction[19,20] have, in fact, been unsuccessful. In the present experiment, we have therefore investigated fission of Ac and Ra isotopes for which the outer barrier is presumably the higher one. In order to obtain sufficiently low excitation energies, we have investigated fission of ^{226}Ac, ^{227}Ac, ^{228}Ac and of ^{225}Ra, ^{227}Ra induced by the reactions (^{3}He,t), (^{3}He,d), (^{3}He,α), (d,p), on a ^{226}Ra target respectively. It has been proved [21] by cross bombardments and by a comparison with neutron induced fission that indeed direct reactions provide a reliable tool for determining fission thresholds.

2. EXPERIMENT AND DATA ANALYSIS

The experiments were carried out with 23.5-MeV ^{3}He and 18-MeV d beams from the Munich MP accelerator on a 50 μg/cm^2 ^{226}Ra target evaporated on a 20 μg/cm^2 carbon backing. The outgoing light particles from the direct reactions were identified by a ΔE - E telescope mounted at 108° with respect to the beam axis. In coincidence with these, the fission fragments were

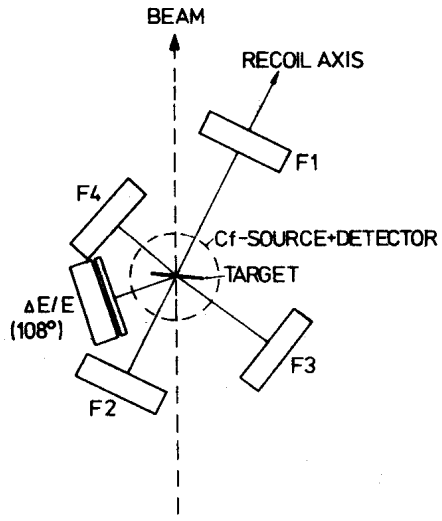

FIG. 1. Diagram of the detector arrangement. The dashed circle indicates the position of a ^{252}Cf source mounted on a Si-detector above the reaction plane for on-line calibration and stabilization of the fission detectors F1 to F4.

measured in two pairs of semiconductor detectors at approximately 0° and 90° with respect to recoil axis in very close geometry. A geometrically correct diagram of the detector arrangement is given in fig.1. On-line calibration and stabilization of the fragment detectors was done by additional coincidences with a further detector placed behind a ^{252}Cf spontaneous fission source. Fast-slow techniques with constant fraction triggers were used throughout, with pile-up rejection in addition for the ΔE-detector. The pulses from the 6 detectors and their time relationship were digitized in 7 ADCs, fed into the Munich PDP8/10 computer system and stored event-by-event on magnetic tape. The incoming data were sorted into four types of events: (a) ΔE-E telescope coincidences; (b) triple coincidences of ΔE/E with either F2 or F4, the closer fission fragment detectors in each direction; (c) quadruple coincidences of ΔE/E with either F1/F2 or F3/F4; (d) events in each of the fission detectors F1 to F4 in coincidence with the ^{252}Cf detector mentioned above.

The data were then analyzed on-line according to excitation energy of the final nucleus, fragment mass and total kinetic energy using the Schmitt calibration method[22] and including corrections for recoil effects, prompt neutron emission and target absorption. Chance coincidences could be exactly corrected for using the time spectra of the coincidences and the singles particle energy spectra.

From the data, the fission anisotropies $\sigma_f(0°)/\sigma_f(90°)$ and the fission probabilities

$$P_f = \frac{\sigma(^3He,pf)}{\sigma(^3He,p)} = \frac{\Gamma_f}{\Gamma_n} \qquad \text{for } \Gamma_f \ll \Gamma_n$$

(and equivalent for the other reactions used) were determined as a function of excitation energy. The denominator σ (^{3}He,p) is obtained from the ΔE-E singles but must be corrected for contaminants from the C-target backing and, specifically in this case, for break-up of the ^{3}He particle into p+p+n in the Coulomb field of the target nucleus which was investigated separately with coincidences between pairs of ΔE/E telescopes. The break-up correction influences only the data obtained for the highest excitation energies. In all cases, the "true" singles spectrum has been checked by additional runs with ^{3}He and d on ^{238}U, assuming that the fission-particle coincidence spectra represent the shape of the reaction singles spectrum, since Γ_f / Γ_n is nearly constant over a wide energy region for the corresponding compound nuclei [21,23] (taking into account the second-chance fission effects and small differences in the Coulomb field between Ra and U). Throughout the paper, the indicated error bars refer to statistical errors only; the systematic error is of the order of 20%.

For ^{226}Ra(^{3}He,α)^{225}Ra$\rightarrow$f a further correction must be applied for ternary fission of the ^{229}Th compound nucleus formed after ^{3}He capture. A good quantitative estimate of this correction can be obtained from the observation of α-particle-fission coincidences in the reaction d+^{226}Ra, for which the reaction ^{226}Ra(d,α)^{224}Fr$\rightarrow$f is ruled out energetically for the deuteron energy used. The shape of this α spectrum as well as its relative yield are in agreement with similar data on ^{252}Cf spontaneous ternary fission [24]. For the total energy range covered in the experiment, the total amount of this correction is about 20% of the observed events with an estimated relative error of 0.2 included in the error bars for the ^{225}Ra data.

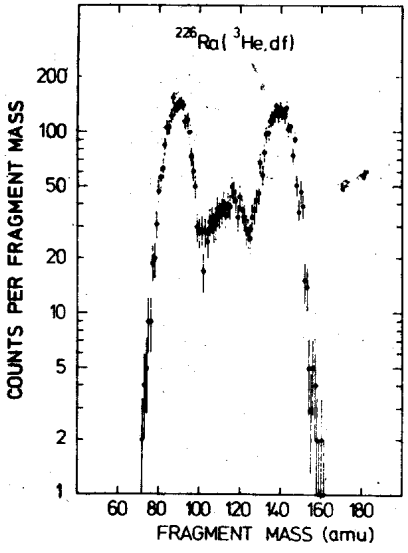

FIG. 2. Fragment mass distribution for fission of ^{227}Ac at excitation energies between 7 and 13 MeV.

The fission probabilities and fragment anisotropies were analyzed both for events of type (b), and for the asymmetric and symmetric component separately (using coincidences of type (c)). Fig.2 shows, for example, the fragment mass spectrum for fission of ^{227}Ac at 0° corresponding to excitation energies between 7 and 13 MeV. The symmetric component was determined from a narrow mass window (in this case $105 < A < 123$) and its corresponding yield multiplied by a scale factor (~ 1.4) transforming the window observed to the area corresponding to a symmetric mass distribution with Gaussian shape [9]. Because of the steeper angle with respect to the target surface for the fission fragments detected, the pair of detectors F1/F2 had a better mass resolution, i.e. no tails from the asymmetric yield in the symmetric window; for F3/F4 a small correction (3% of the asymmetric yield) for such tails had to be subtracted. The sum of the counts for the symmetric and asymmetric components observed in correlated detector pairs F1/F2 or F3/F4 were normalized to the corresponding number of counts observed in F2 or F4 alone, to avoid errors from misalignment of the detectors.

For the two nuclei investigated with the highest statistical accuracy (^{227}Ac and ^{228}Ac) the data were also completely analyzed with respect to the correlated three parameters: nuclear excitation energy, fragment kinetic energy and fragment mass.

3. FISSION PROBABILITY FOR ASYMMETRIC AND SYMMETRIC FISSION

The mass distribution for ^{227}Ac for $7 \leq E_x \leq 13$ MeV as given in fig.2 shows a triple humped curve with clear minima between the three mass yield peaks. Since second-chance fission is excluded here for energetical reasons, we can conclude that both fission modes really occur in the same nucleus, contrary to speculations that one of them is due to fission of another isotope after neutron emission from the originally excited nucleus.

Figs 3 and 4 show fission probabilities and fragment anisotropies as a function of excitation energy in the fissioning nuclei ^{226,227,228}Ac and ^{225,227}Ra, respectively, separately for the symmetric and asymmetric fission modes. In all cases the data presented for the (in most cases dominant) asymmetric component were obtained by subtraction of the curve indicated in the figs. for the symmetric component from the data points for total fission which were measured with higher statistical accuracy (events of type (b)). Only for ^{225}Ra in fig.4 the total fission probability is given in addition, for clarity displaced by a factor of 10.

Several interesting features are directly visible in figs. 3 and 4.

1. Most important, symmetric and asymmetric fission appear, in fact, to be associated with different fission barriers; for all cases except ^{225}Ra the symmetric barriers appear to be higher than the asymmetric ones. This is definitely true for ^{227}Ac and ^{228}Ac, the two cases with the highest statistical accuracy (8.5 MeV compared to 7.3 for ^{227}Ac, 9.2 compared to 7.2 for ^{228}Ac respectively). In these cases, the upper limit for a

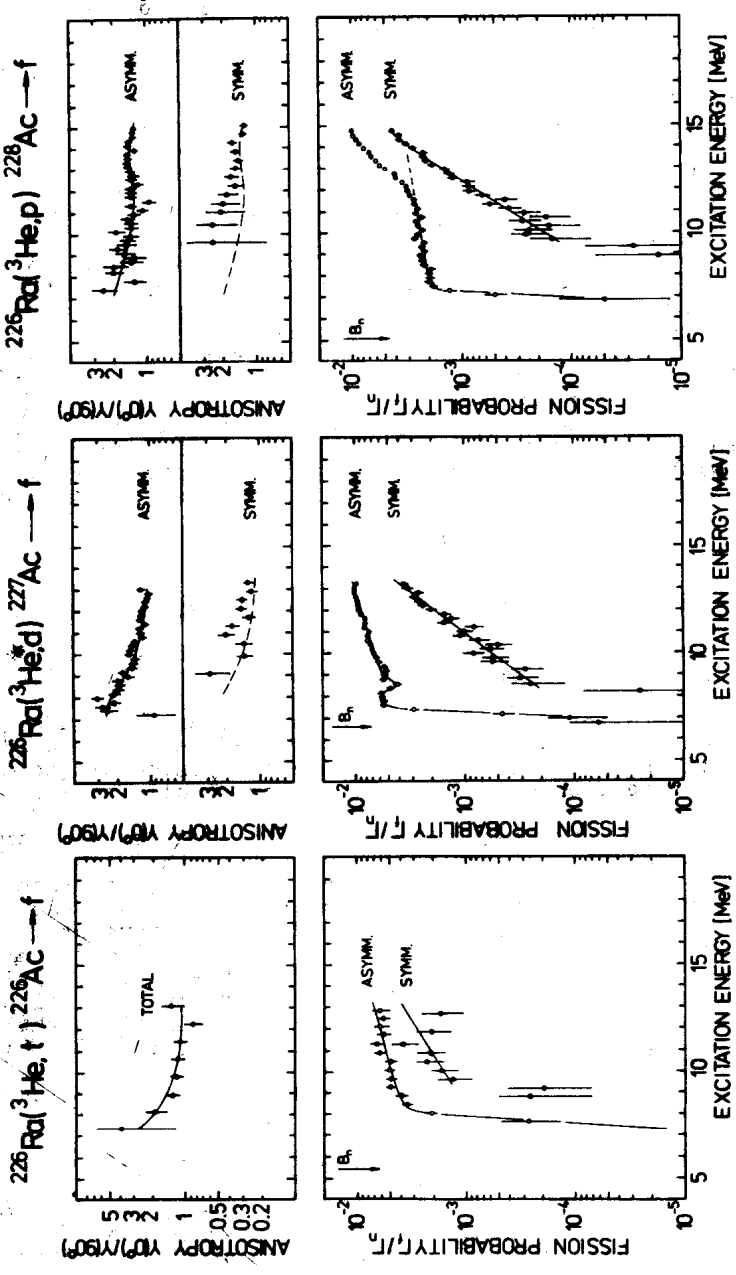

FIG. 3. Fission probabilities and fragment anisotropies for ^{226}Ac, ^{227}Ac and ^{228}Ac as a function of the excitation energy in the fissioning nuclei. Arrows mark the neutron binding energies. Solid lines fitting the asymmetric anisotropy data are repeated as dashed lines in the field showing the symmetric data.

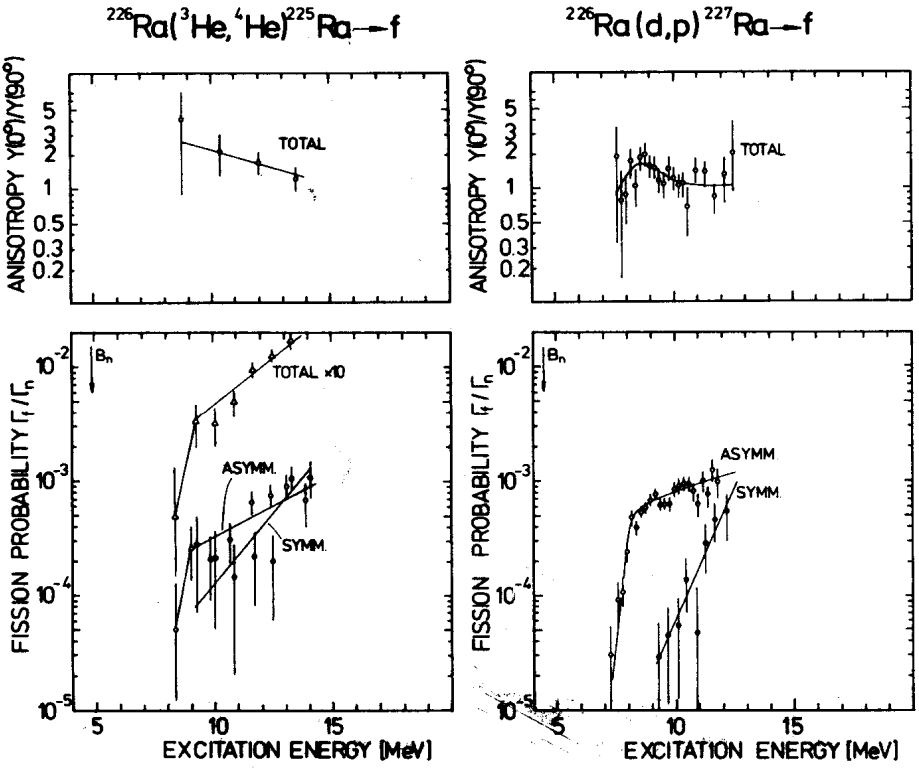

FIG. 4. Fission probabilities and fragment anisotropies for ^{225}Ra and ^{227}Ra as a function of the excitation energy in the fissioning nuclei. Arrows mark the neutron binding energies.

possible symmetric yield averaged over the region between the two thresholds relative to the symmetric yield just above the symmetric threshold is 6% (95% confidence limit). The fragment angular anisotropies also seem to be different for the two mass components; the dashed line in the plots for symmetric fission (top of fig.3) marks the anisotropy for the asymmetric component. This difference further supports the interpretation of the different threshold behaviour as really being due to separate barriers.

2. Following the well-known trend at the lower-Z actinides, the atomic number of the fissioning nucleus appears to have a predominant influence on the total fission probability. From Ra to Ac, adding one single proton increases the fission probability near the threshold by almost a factor of 10. Nevertheless, the absolute fission probabilities, especially for symmetric fission, are extremely small, which, of course, presents the major difficulty of these experiments.

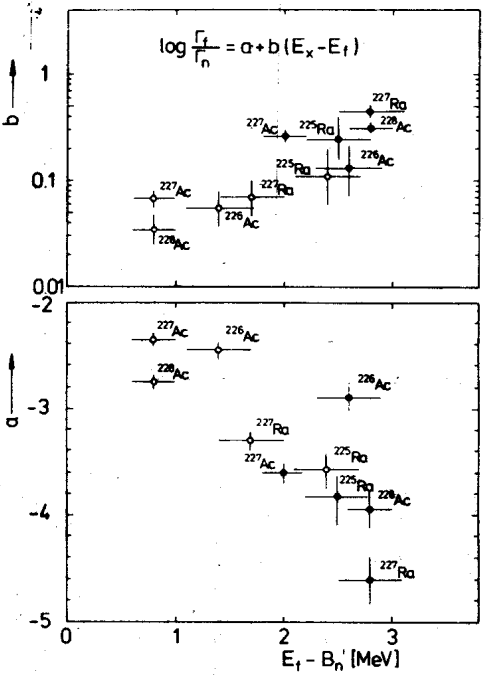

FIG. 5. Intercept a and slope b of the function $\log(\Gamma_f/\Gamma_n) = a + b(E_x - E_f)$ as a function of $E_f - B_n'$ for all nuclei investigated, plotted separately for the asymmetric (open circles) and symmetric (filled circles) components. The quantities E_x, E_f and B_n' are explained in the text.

3. The competition of symmetric and asymmetric fission seems to be governed more by the neutron number. Clearly, both for Ra and Ac the nuclei investigated with the smallest neutron numbers (^{225}Ra and ^{226}Ac) reveal the biggest relative contributions of symmetric fission.

4. The fission probability for both the symmetric and asymmetric component rises exponentially with increasing excitation energy, generally for the symmetric component much steeper than for the asymmetric one. In the logarithmic plots of figs.3 and 4, the slope of the fission probability $\partial(\log(\Gamma_f/\Gamma_n))/\partial E_x$ for both fission modes remains constant for at least 5 MeV above the barrier (the increase above the dotted line for ^{228}Ac in fig.3 is caused by the onset of second-chance fission) and is much smaller than expected on the basis of simple statistical model considerations [25]. However, it seems to be influenced by the same parameters used in ref. [25] to describe the statistical aspects of neutron evaporation vs. fission competition. Fig.5 shows the slope b and the intercept a of the function $\log(\Gamma_f/\Gamma_n) = a+b(E_x-E_f)$ as a function of E_f-B_n', E_f being the fission barrier and B_n' the neutron binding energy of the daughter nucleus after neutron evaporation, corrected for even-odd neutron number